

# Charge-Transfer Complex of 4-Cyano-5,6-diphenylpyridazine-3(2)selenone with Picric Acid: Infrared, Raman, Spectrophotometric, and Photostability Studies<sup>1</sup>

Moamen S. Refat<sup>a,b</sup> and Shams H. Abdel-Hafez<sup>a,c</sup>

<sup>a</sup> Department of Chemistry, Faculty of Science, Taif University, 888 Taif, Kingdom Saudi Arabia  
e-mail: msrefat@yahoo.com

<sup>b</sup> Department of Chemistry, Faculty of Science, Port Said, Port Said University, Egypt

<sup>c</sup> Chemistry Department, Faculty of Science, Assiut University, Assiut 71516, Egypt

Received January 9, 2014

**Abstract**—Change transfer complex of 4-cyano-5,6-diphenylpyridazine-3(2)selenone (CDS) was obtained by reacting of CDS with picric acid. The structure was confirmed by a number of spectral (IR, Raman, UV-Vis) methods. The activation parameters  $\Delta E$ ,  $\Delta H$ ,  $\Delta S$ , and  $\Delta G$  were obtained from the DTG diagrams using Coats-Redfern and Horowitz-Metzger methods. The photostability of 4-cyano-5,6-diphenylpyridazine-3(2)selenone (CDS) and its charge-transfer complex doped in polymethyl methacrylate (PMMA) matrix exposed to UV-Vis radiation was studied.

**DOI:** 10.1134/S1070363214020315

## INTRODUCTION

It is well known that the selenium compounds are used in medical applications and also play an important role in the production of commercial solar cells. The stability of solar cells and polymer matrices has been drawing attention for many years, that lead to enhancing the prospects of solar cell conversion. In addition, selenium compounds are used in paints, dyes, glass, electrical, rubber, insecticide industries [1] and photocell devices [2]. Heterocyclic annulated pyridazines continue to attract considerable attention, which mainly arises from the large variety of interesting pharmacological activities of herbicides, insecticides and fungicides containing pyridazine moiety [3, 4]. On the other hand, the current interest in selenium containing heterocycles is a result of their chemical properties and biological activities [5–9]. In addition, numerous recent publications deal with the pharmaceutical potential of selenium compound [10–15] and therefore new efficient syntheses are an attractive goal of chemical research [16–19]. Charge transfer interactions between electron donors and acceptors are generally associated with the formation of intensely

colored charge-transfer (CT) complexes which absorb radiation in the visible region [20]. Molecular complexation and structural recognition are important processes in biological systems; for example, drug action, enzyme catalysis and ion transfers through lipophilic membranes all involve complexation [21]. Mulliken suggested that the formation of molecular complexes from two aromatic molecules can arise from the transfer of an electron from a  $\pi$ -molecular orbital of a Lewis base to a vacant  $\pi$ -molecular orbital of a Lewis acid, with resonance between this dative structure and the no-band structure stabilizing the complex [22]. Mulliken also noted the possibility of complex formation through the donation of an electron from a non-bonding molecular orbital in a Lewis base to a vacant  $\pi$ -orbital of an acceptor ( $n-\pi$ ) [23] with resonance stabilization of the combination. Charge-transfer complexes are known to take part in many chemical reactions like addition, substitution and condensation [24–26]. Photostability of the polymers is one of their most important properties. To solve the problem of polymer stabilization, a number of different stabilizers have successfully been applied [27]. Among them, selenium compounds-UV absorbers are of great interest due to their high photostabilizing efficiency. They are transparent to visible light and are supposed

<sup>1</sup> The text was submitted by the authors in English.

to dissipate the absorbed energy in a harmless manner, i.e. to convert the absorbed photon energy into heat without being chemically affected [28]. The aim of the present paper was to synthesize, investigate thermal behavior and photostability of 4-cyano-5,6-diphenylpyridazine-3(2)selenone (CDS) (Fig. 1), picric acid (PA) complex. The chelation behavior of CDS toward picric acid acceptor was investigated and the data are confirmed with their molar conductance and spectrophotometric measurements. The thermal decomposition of CDS-PA complex was used to speculate the structure, also the thermal stability studies are essential feature in relation to their application as highly photostable materials. The determination of association constant ( $K$ ), molar extinction coefficients ( $\epsilon$ ) and oscillator strength ( $f$ ) were carried out. Herein, modification has led to increasing the photostability of the CDS. In this paper, the effect of sun radiation on the physicochemical properties of charge-transfer adduct as a solar collector model was investigated including behavior of the selenone moiety chelating stability and release profiles.

#### EXPERIMENTAL

All chemicals and solvents used were of fine grade. The 4-cyano-5,6-diphenylpyridazine-3(2)selenone (CDS) was prepared as previously described [29]. Picric acid (PA) and Poly(methylmethacrylate) (PMMA) were purchased from Merck Chemical Company and were also used as received.

The elemental analyses of the carbon, hydrogen and nitrogen contents were performed using a Perkin-Elmer CHN 2400 instrument. The electronic absorption spectra of methanolic solutions of the CDS, PA and CDS-PA complex were recorded over a wavelength range of 200–800 nm using a UV-Vis double-beam JASCO-V-670 spectrophotometer. The instrument was equipped with a quartz cell with a 1.0 cm path length. The molar conductivities of freshly prepared  $1.0 \times 10^{-3}$  mol/cm<sup>3</sup> DMSO solutions were measured using Jenway 4010 conductivity meter. The mid-infrared (IR) spectra (KBr discs) within the range of 4000–400 cm<sup>-1</sup> were recorded on a Bruker FT-IR spectrophotometer with 30 scans at 2 cm<sup>-1</sup> resolution, while Raman laser spectra were measured on a Bruker FT-Raman with 50 mW laser. Thermogravimetric analysis (TG/DTG) was performed under static nitrogen atmosphere between room temperature and 800°C at a heating rate of 10°C/min using a Shimadzu TGA-50H thermal analyzer.

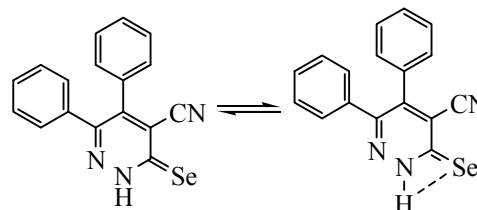


Fig. 1. Structure of 4-cyano-5,6-diphenylpyridazine-3(2)-selenone.

**Photostability.** Solar simulator 250 Watt xenon arc lamp was used, which had the same spectrum as sun. The degradation of samples was studied by analyzing the UV-Vis absorption spectra. The photostability was calculated by dividing the absorbance after exposure to light by that before exposure.

**Synthesis of 4-cyano-5,6-diphenylpyridazine-3(2)-selenone (CDS).** A mixture of chloropyridazine (2.91 g, 10 mmol), “metallic” selenium (1 g, 12 mmol) and sodium borohydride (1.2 g, 32 mmol) was refluxed in 50 mL of ethanol for 5 h. The mixture was cooled and poured into ice/HCl. The yellow-to-brown solid separated out was filtered off, dried and recrystallized from ethanol. <sup>13</sup>C NMR spectrum (DMSO-*d*<sub>6</sub>, 75 MHz),  $\delta$ , ppm: 158.90 (C=N of pyridazine), 155.98, 144.84, 142.08, 134.86, 134.08, 129.99, 129.37, 128.92, 128.30, 127.88 (aryl), 118.02 (CN), 114.78 (C–CN); mass spectrum of CDS has molecular ion peak at  $m/z$ , % 336 ( $M^+$ , 45%) and the other important fragments were observed at 337 [ $M + 1$ ]<sup>+</sup> 87%, 338 [ $M + 2$ ]<sup>+</sup>, 19%, (265) 60%, (178) 100%, (140) 50%, (77) 80%.

**Synthetic solid powder of CDS-PA charge-transfer complex.** The solid charge-transfer product of CDS and PA was prepared by mixing 1 mmol amounts of CDS and PA in 25 mL of methanol. The mixture was stirred for 30 min at 50°C and allowed to evaporate slowly at room temperature, which resulted in the precipitation of the solid greenish brown charge-transfer complex. The separated complex was filtered off, washed well with little amounts of methylene chloride and then collected and dried under vacuum over anhydrous calcium chloride for 24 h.

**Preparation of polymer sheet.** Both poly(methyl methacrylate) (PMMA) grains and CDS or its PA complex were dissolved in methylene chloride and mixed using a magnetic stirrer. The homogenous mixture was poured into a glass Petri dish and allowed to dry.

**Table 1.** Analytical and physical data for CDS and CDS-PA charge transfer complex

| Complex<br>( $M_w$ , g/mol) | Color          | $\Delta m$<br>( $\Omega^{-1} \text{ cm}^{-1} \text{ mol}^{-1}$ ) | Found, % |      |       | Calculated, % |      |       | Yield, % |
|-----------------------------|----------------|--|----------|------|-------|---------------|------|-------|----------|
|                             |                |  | C        | H    | N     | C             | H    | N     |          |
| CDS (336.25)                | Brown          | 21   | 60.72    | 3.30 | 12.50 | —             | —    | —     | 90       |
| CDS-PA (580.39)             | Greenish brown | 56   | 49.54    | 2.88 | 14.33 | 49.67         | 2.95 | 14.48 | 92       |

**Table 2.** Spectrophotometric data for the CDS-PA complex

| Complex | CT-absorption,<br>nm | $E_{CT}$ , eV | $K$ , $\text{L mol}^{-1}$ | $\epsilon_{\text{max}}$ , $\text{L mol}^{-1} \text{ cm}^{-1}$ | $f \times 10^2$ | $\mu$ | $I_p$ | $R_N$ | $\Delta G^0$ (25°C), $\text{kJ mol}^{-1}$ |
|---------|----------------------|---------------|---------------------------|---|-----------------|-------|-------|-------|---|
| CDS-PA  | 348                  | 3.57          | $22 \times 10^4$          | $8 \times 10^4$   | 0.43            | 61    | 10.16 | 0.928 | −29.976                                   |

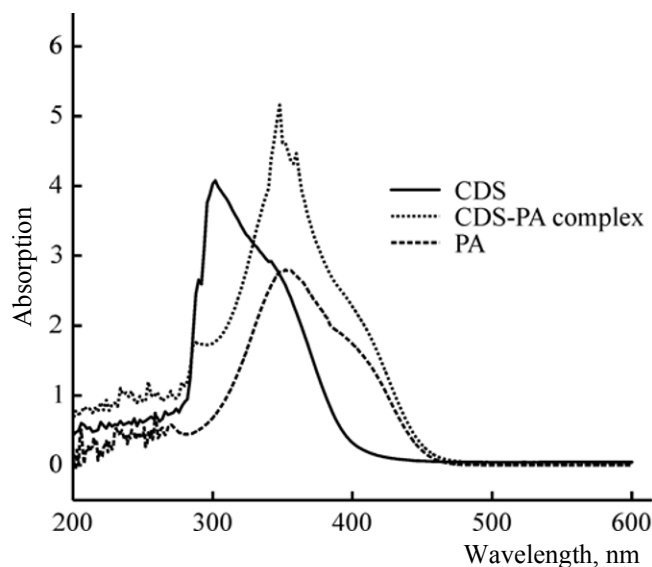
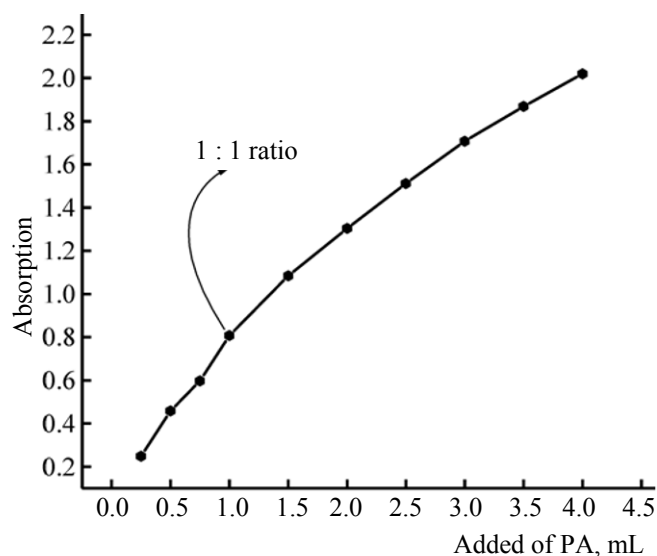
## RESULTS AND DISCUSSION

### Assignments of analytical and conductivity data.

The molecular weights, molecular formula, conductance, yield, color as well as carbon, hydrogen and nitrogen contents of CDS charge-transfer complex are listed in Table 1. The elemental analysis supports 1 : 1 (CDS : PA) stoichiometry. The complexation process occurs via  $-\text{CN}$  group of CDS moiety toward  $-\text{OH}$  of accepting center. The molar conductance values ( $21$  and  $56 \Omega^{-1} \text{ cm}^{-1} \text{ mol}^{-1}$  for CDS and CDS-PA complex, respectively) indicate that the charge-transfer complex has slightly electrolytic nature, assigned to the formation of positive and negative dative anions under the donor-acceptor chelation [30].

**Spectrophotometric and physical spectroscopic data.** The UV-Vis spectra were measured in  $\text{CH}_3\text{OH}$ .

The charge-transfer complex was formed by adding  $x$  mL of  $5.0 \times 10^{-4}$  M PA solution ( $x = 0.25, 0.50, 0.75, 1.00, 1.50, 2.00, 2.50$ , and  $3.00$  mL) to  $1.00$  mL of  $5.0 \times 10^{-4}$  M CDS solution. The total volume of each sample was adjusted to  $5$  mL with methanol. CDS concentration was kept fixed at  $1.00 \times 10^{-4}$  M, while PA concentration was varied over the range of  $0.25 \times 10^{-4}$  M to  $3.00 \times 10^{-4}$  M, producing CDS : PA ratios in the range from  $1 : 0.25$  to  $1 : 3.00$ . The electronic absorption spectra of the  $1 : 1$  ratio in methanol as well as free CDS are shown in Fig. 2. The spectra reveal characteristic absorption bands which are not present in the spectra of free reactants. This band at  $348$  nm is assigned to the CT-complex formed in the reaction of CDS with PA. Photometric titration curve based on this characteristic absorption band is given in Fig. 3. This curve was obtained according to known methods

**Fig. 2.** Electronic absorption spectra of CDS, PA and CDS-PA charge-transfer complex.**Fig. 3.** Photometric titration curve of CDA-PA system.

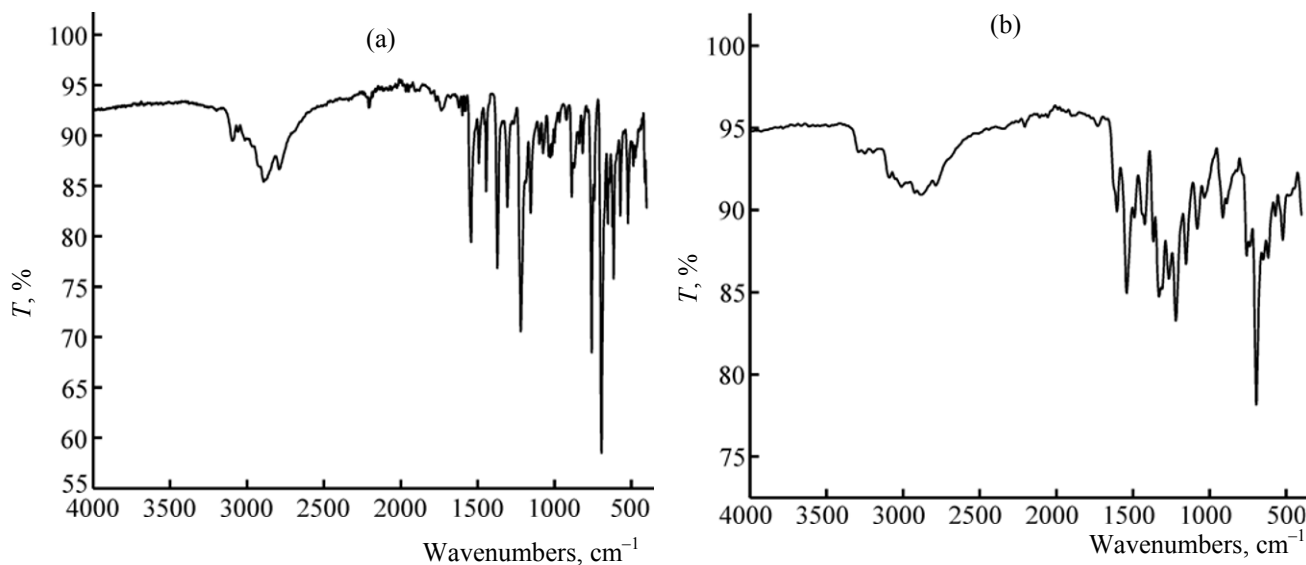


Fig. 4. Infrared spectra of (a) CDS free donor and (b) CDS-PA complex.

[31] by plotting of the absorbance against the PA volume added as  $\pi$ -acceptor. The equivalence points shown in this curve clearly indicate that CT-complex formed between CDS and PA has 1 : 1 molar ratio. It was of interest to observe that the solvent has a pronounced effect on the spectral intensities of the formed charge-transfer complex. The 1 : 1 modified Benesi-Hildebrand equation [32] was used in the calculations (1).

$$\frac{C_a^0 C_d^0}{A} = \frac{1}{K\varepsilon} + \frac{C_a^0 + C_d^0}{\varepsilon}, \quad (1)$$

where  $C_a^0$  and  $C_d^0$  are the initial concentrations of the picric acid and CDS, respectively,  $K$  is a formation constant,  $\varepsilon$  is a molar extinction coefficient, and  $A$  is the absorbance of the definite band 348 nm for CDS-PA system, respectively. The  $(C_a^0 C_d^0)/A$  values are plotted against the corresponding  $C_a^0 + C_d^0$  values, straight line was obtained with a slope of  $1/\varepsilon$  and intercept of  $1/K\varepsilon$ . The oscillator strength  $f$  was obtained from the approximate formula given in Eq. (2) [33]:

$$f = (4.319 \times 10^{-9}) \varepsilon_{\max} \nu_{1/2}, \quad (2)$$

where  $\nu_{1/2}$  is the band-width for half-intensity in  $\text{cm}^{-1}$ . The oscillator strength value together with the corresponding dielectric constants,  $D$ , of the solvent used are given in Table 2.

CDS-PA Complex shows high values of both the equilibrium constant ( $K$ ) and the extinction coefficient ( $\varepsilon$ ). This high value of  $K$  reflects the high stability of the CDS complex as a result of the expected high

donation of the CDS consequently high value of  $\varepsilon$  which is known to have a high absorptivity values [34–36]. The transition dipole moment ( $\mu$ ) of the CDS complex (Table 2) have been calculated from Eq. (3) [37]:

$$\mu = 0.0958 [\varepsilon_{\max} \nu_{1/2} / \nu_{\max}]^{1/2}, \quad (3)$$

where  $\nu_{1/2}$  is the bandwidth at half-maximum of absorbance,  $\varepsilon_{\max}$  and  $\nu_{\max}$  are the extinction coefficient and wavenumber at maximum absorption peak of the CT complexes, respectively. The ionization potential ( $I_p$ , eV) of the free CDS donor was determined from the CT energies of the CT band of its PA complex with different  $\pi$ -acceptors using the following Aloisi and Piganatro [38] relationships.

$$I_p = 5.76 + 1.53 \times 10^{-4} \nu_{\text{CT}}. \quad (4)$$

$E_{\text{CT}}$  is the energy of the CT of the CDS complex, the energy of the  $\pi-\sigma^*$ ,  $n-\sigma^*$ ,  $\pi-\pi^*$  or  $n-\pi^*$  interaction ( $E_{\text{CT}}$ , eV) is calculated using Eq. (5) [39]:

$$E_{\text{CT}} = (h\nu_{\text{CT}}) = 1243.667 / \lambda_{\text{CT}}, \quad (5)$$

where  $\lambda_{\text{CT}}$  is the wavelength of the characteristic complexation band, nm. Determination of resonance energy ( $R_N$ ), from Briegleb and Czékalla [40] derived the relation given in Eq. (6):

$$\varepsilon_{\max} = 7.7 \times 10^{-4} / (h\nu_{\text{CT}} / R_N - 3.5), \quad (6)$$

where  $\varepsilon_{\max}$  is the molar extinction coefficient of the complex at the maximum CT absorption,  $\text{L mol}^{-1} \text{cm}^{-1}$ ,  $\nu_{\text{CT}}$  is the frequency of the CT peak, and  $R_N$  is the resonance energy of the complex in the ground state,

**Table 3.** Kinetic thermodynamic data of CDS and CDS-PA complex

| Complexes | DTG <sub>max</sub> /°C | $\Delta E$ ,<br>kJ mol <sup>-1</sup> |    | $\Delta H$ ,<br>kJ mol <sup>-1</sup> |    | $\Delta S$ ,<br>J mol <sup>-1</sup> K <sup>-1</sup> |     | $\Delta G$ ,<br>kJ mol <sup>-1</sup> |     | $r$    |        |
|-----------|------------------------|--------------------------------------|----|--------------------------------------|----|---|-----|--------------------------------------|-----|--------|--------|
|           |                        | CR                                   | HM | CR                                   | HM | CR  | HM  | CR                                   | HM  | CR     | HM     |
| CDS-PA    | 305                    | 94                                   | 97 | 90                                   | 94 | -50   | -40 | 110                                  | 108 | 0.9860 | 0.9820 |
| CDS       | 259                    | 63                                   | 68 | 60                                   | 65 | -105  | -86 | 96                                   | 95  | 0.9740 | 0.9770 |

which obviously is a contributing factor to the stability constant of the complex (a ground state property). The value of  $R_N$  for the CDS-PA complex is given in Table 2. The standard free energy changes of complexation ( $\Delta G^0$ ) were calculated from the association constants by Eq. (7) [41]:

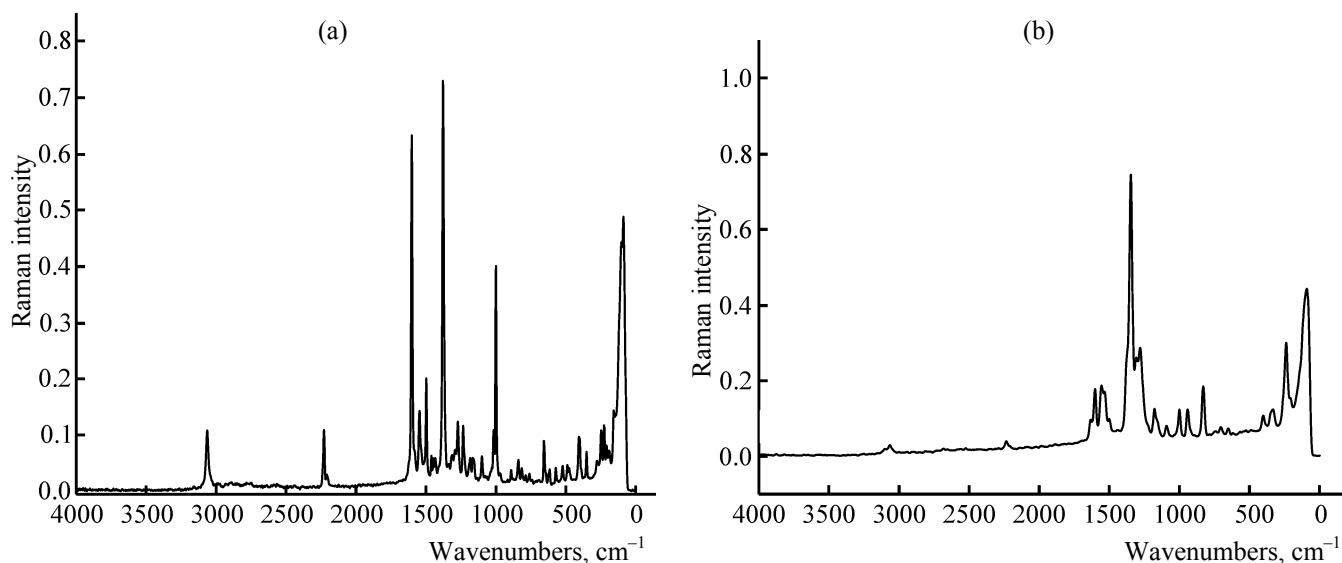
$$\Delta G^0 = -2.303RT \log K_{CT}, \quad (7)$$

where  $\Delta G^0$  is the free energy change of the complexes (kJ mol<sup>-1</sup>),  $R$  is the gas constant (8.314 J mol<sup>-1</sup> K),  $T$  is the temperature in Kelvin, and  $K_{CT}$  is the association constant of the complexes (L mol<sup>-1</sup>) in respective solvent at room temperature, the value thus calculated is represented in Table 2. The data of  $\Delta G^0$  has a negative value according to the higher values of formation constant, and thus the formation of CDS charge-transfer complex is exothermic reaction.

**FT-IR and Raman spectra assignments.** The infrared and Raman laser spectra of CDS and its PA charge-transfer complex are shown in Figs. 4 and 5, respectively. The vibrational spectra of CDS contains several characteristic peaks for which assignments have been made on the basis of location and inten-

sities. The vibration motions of characteristic bands can be summarized upon stretching and bending motions of function groups.

**N–H vibration motions.** In pyridazine, the free N–H group absorbed at 3490–3200 cm<sup>-1</sup> [42] while the associated group has a stretching vibration motion in CDS free donor at 3096 cm<sup>-1</sup>. This is due to the intermolecular hydrogen bond formed between N–H (pyridazine moiety) and selenium of C=Se group (Fig. 1). Thus, in case of free CDS, the band observed at 3096 and 3065 cm<sup>-1</sup> in FT-IR and Raman spectra, respectively, have been assigned to N–H stretching band frequency. On the other hand, upon charge-transfer complexation between CDS and picric acid, the medium-to-weak bands presented at 3304 and 3197 cm<sup>-1</sup> in FT-IR spectrum attributed to the associated of C=NH group via deprotonated picric acid. The place of absorption concerning N–H hetero aromatic moiety depend on the degree of hydrogen bonding between the atoms and hence upon the physical state of the compound or polarity [43]. In the FT-IR and Raman spectra of CDS-PA complex, a medium intensity band observed at 1608 cm<sup>-1</sup> is

**Fig. 5.** Raman laser spectra of (a) CDS free donor and (b) CDS-PA complex.

assigned to new associated C=NH group that absented in the free CDS donor.

**C–H vibration motions.** The heterocyclic compounds have few stretching vibration motion of C–H within range of 3014–2888  $\text{cm}^{-1}$  [44]. CDS-PA complex has not massive change in the C–H vibration motions. The C–H in-plane bending vibrations in phenyl pyridazine nucleus have many bands in the region of 1300–1000  $\text{cm}^{-1}$  at 1310, 1218, 1152, 1102, 1077, and 1028  $\text{cm}^{-1}$  and 1335, 1227, 1268, 1161, and 1035  $\text{cm}^{-1}$  for CDS free donor and CDS-PA complex [45], respectively. The C–H out-of-plane bending vibration gives strong-to-medium bands within region of 1000–600  $\text{cm}^{-1}$  [45]. The C–H out-of-plane bending for CDS and CDS-PA was observed at 886, 811, 762, 695, 654, and 612  $\text{cm}^{-1}$  and 911, 762, 694, and 620  $\text{cm}^{-1}$ , respectively. Accordingly, in CDS free compound and CDS-PA complex, the C–H in-plane bending and C–H out-of-plane bending vibrations were observed at 1271, 1234, 1161, and 1098  $\text{cm}^{-1}$  and 997, 834, and 652  $\text{cm}^{-1}$  for CDS free compound and at 1289, 1179, 1098, and 1006  $\text{cm}^{-1}$  and 942 and 834  $\text{cm}^{-1}$  for CDS-PA complex, respectively.

**C $\equiv$ N vibration motions.** The absorption of triple bond between carbon and nitrogen (nitrile group) normally occurs at 2207 and 2226  $\text{cm}^{-1}$  [46] in FT-IR and Raman spectra, respectively. In the association of CDS-PA complex, the stretching vibration of C $\equiv$ N was disappeared, due to the loss of nitrile group character and forming imine group as shown in Fig. 1.

**Table 4.** Rate constants/ $k$  of photo-degradation and half life times of doped CDS free donor and CDS-PA complex in PMMA

| Sample      | $k$ , $\text{min}^{-1}$ | $t_{1/2}$ , min |
|-------------|-------------------------|-----------------|
| CDS/PMMA    | $1.74 \times 10^{-4}$   | 3983            |
| CDS-PA/PMMA | $1.35 \times 10^{-4}$   | 5139            |

**Phenyl vibration motions.** For phenyl nucleus, the C=C stretching vibration appears as medium-to-strong band within the range of 1540–1370  $\text{cm}^{-1}$  [45]. In case of CDS free donor, the band corresponding to  $\nu(\text{C}=\text{C})$  vibration motion was observed at 1542, 1493, 1443, and 1368  $\text{cm}^{-1}$  in FT-IR and 1544 and 1498  $\text{cm}^{-1}$  in Raman spectrum. The CDS-PA complex has few absorption bands at 1542, 1484, 1426, and 1368  $\text{cm}^{-1}$  in the FT-IR spectrum and 1562 and 1352  $\text{cm}^{-1}$  in the Raman spectrum assigned to  $\nu(\text{C}=\text{C})$  vibration motion. These results ignore the possibility of  $\pi$ – $\pi^*$  charge-transfer transition from donor to acceptor.

**Se–H vibration motions.** The discussion of stretching vibration motion of  $\nu(\text{Se–H})$  is very important to get knowledge about the structure of CDS compound [selenone ( $\text{C}=\text{Se}$ )  $\leftrightarrow$  selenol ( $\text{Se–H}$ )]. The Se–H bond absorbs in the region of 2300–2280  $\text{cm}^{-1}$  [47]. In both CDS free donor and CDS-PA complex, this vibration band is absent, thus supporting existing of CDS in selenone form. The other fact to support

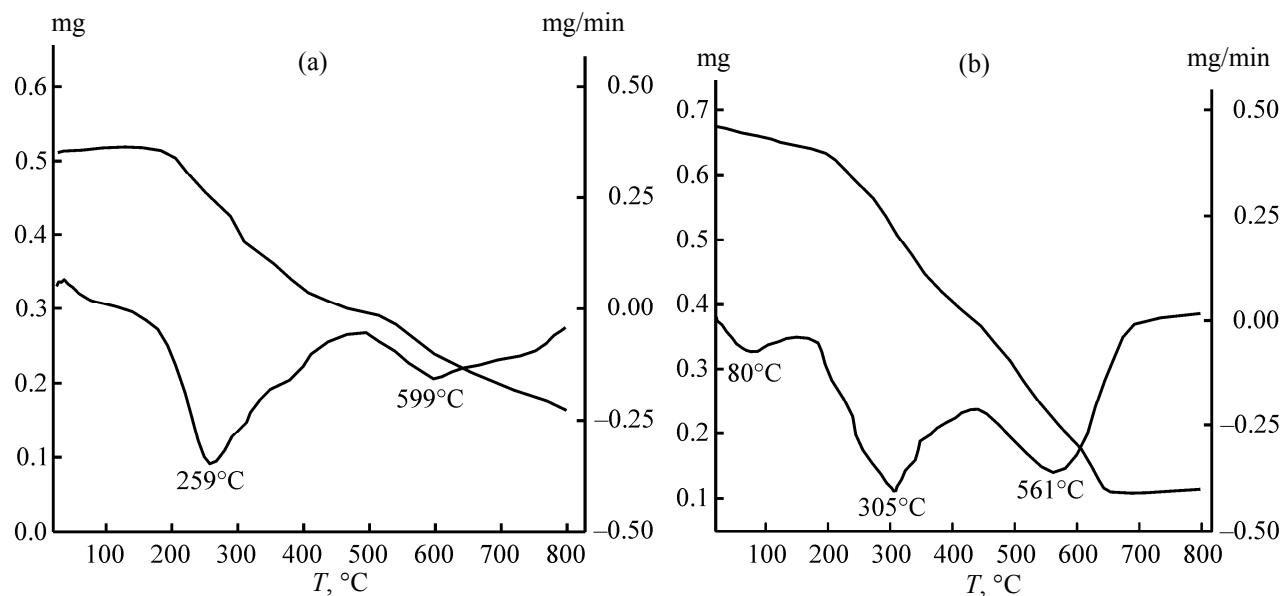
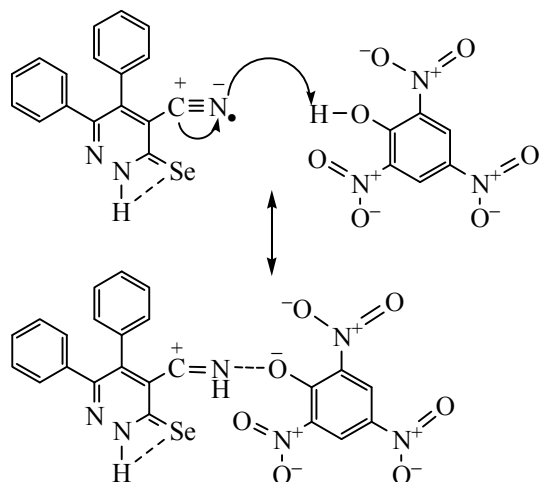


**Fig. 6.** TG-DTG diagram of (a) CDS free donor and (b) CDS-PA complex.

existing CDS in selenone form is the presence of character band within range of 1200–1050 due to  $\nu(\text{C}=\text{Se})$  frequency.

**NO<sub>2</sub> group vibration motions.** The nitro group of picric acid has four vibration motions  $\nu_{\text{as}}(\text{NO}_2)$ ,  $\nu_{\text{s}}(\text{NO}_2)$ ,  $\nu(\text{C}-\text{N})$ , and  $\delta(\text{NCO})$  at 1542, 1335, 911, and 620  $\text{cm}^{-1}$  [48], respectively, in the FT-IR spectrum. Raman spectrum of CDS-PA complex also contains characteristic bands for nitro group at 1562, 1352, 834, and 651  $\text{cm}^{-1}$ .



**Scheme 1.** Suggested mechanism for forming CDS-PA charge-transfer complex.

This suggested mechanism can be explained using picric acid as a catalyst which protonates Lewis base's nitrogen and makes the system more electrophilic. The protonation of the nitrile group gives a charge-transfer

structure that can be redrawn in another resonance form that reveals the electrophilic character of carbon since its carbocation as  $\text{C}\equiv\text{N}^+ + \text{H}^+ \rightarrow {}^+\text{C}=\text{NH}$ .

**Thermal analysis.** Thermal analysis curves (Fig. 6) of the CDS free donor and PA complex show that decomposition takes places in two-to-three stages in the temperature range between 25 and 800°C. The DTG<sub>max</sub> endothermic decomposition stages peaks correspond to the decomposition of the CDS donor and its complex occurred at 259 and 599°C and 80, 305, and 561°C, respectively. The TG/DTG curves of the CDS and CDS-PA complex show a weight loss and mass loss corresponding to the loss of  $\text{C}_{15}\text{H}_{11}\text{N}_3$  organic moiety (found 30.00%, calculated 30.62%) and  $\text{C}_{22}\text{H}_{17}\text{N}_6\text{O}_7$  organic moiety (found 82.00%, calculated 82.62%) for CDS and CDS-PA complex, respectively. The similar final products, formed at 800°C are selenium, contaminated with residual carbon atoms. It is obviously clear that thermal stability of CDS is increasing after forming charge-transfer complex.

**Kinetic studies.** The kinetic parameters for the thermal degradation of the CDS and CDS-PA complex (Fig. 7 and Table 3) namely, activation energy ( $E^*$ ), enthalpy ( $\Delta H^*$ ), entropy ( $\Delta S^*$ ) and free energy of the decomposition ( $\Delta G^*$ ) as well as the pre-exponential factors ( $A$ ), were evaluated graphically using the Coats–Redfern [49] and Horowitz–Metzger [50] methods. The entropy of activation ( $\Delta S$ ), enthalpy of

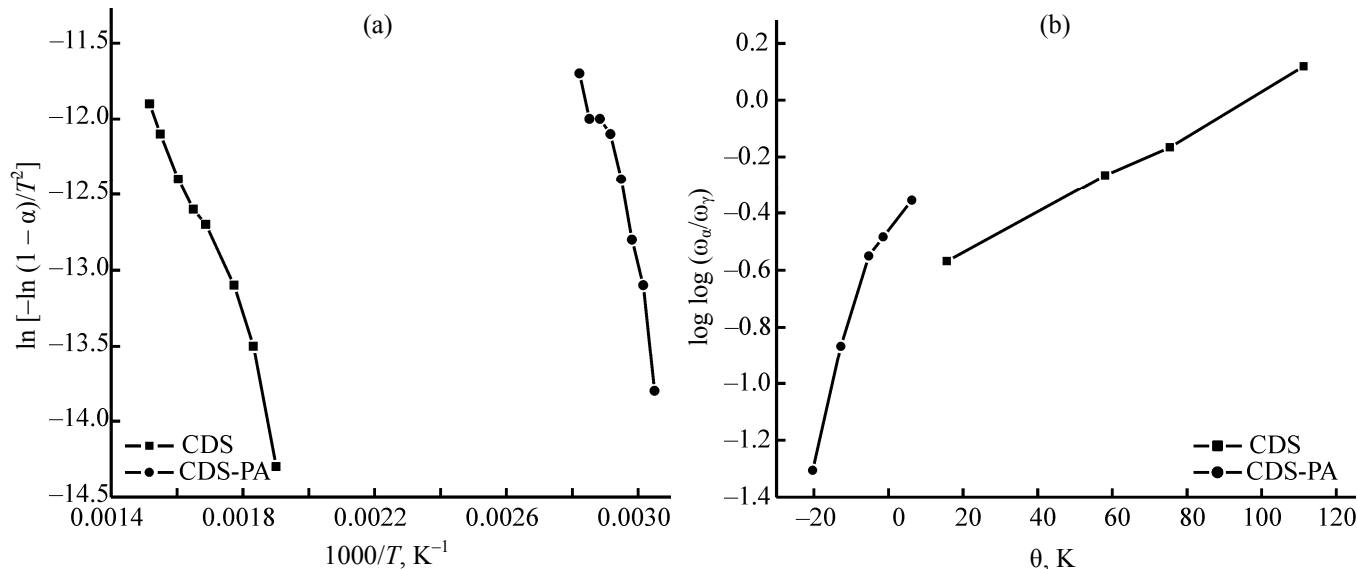


**Fig. 7.** Kinetic thermodynamic diagram of (a) Coats-Redfern and (b) Horowitz-Metzger methods for the CDS free donor and CDS-PA complex.

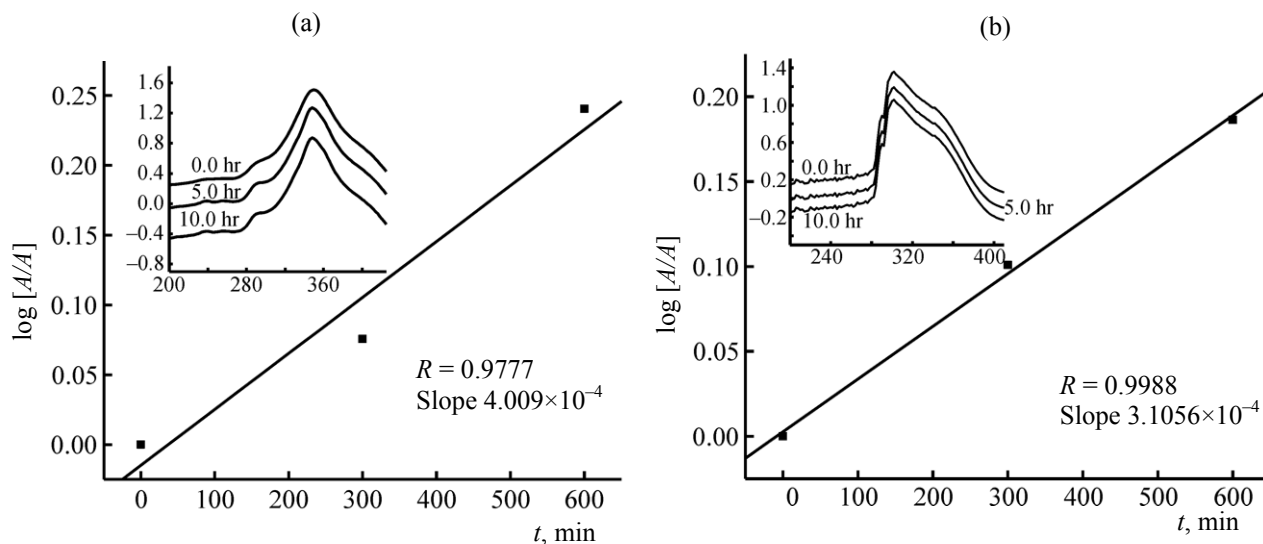


Fig. 8. (a) Photostability of CDS doped in PMMA before and after exposure to UV-Vis light. (b) Photostability of CDS-PA complex doped in PMMA before and after exposure to UV-Vis light.

activation ( $\Delta H$ ) and the free energy changes of activation ( $\Delta G$ ) were calculated using the Eq. (8):

$$\Delta H = E - RT_m; \Delta G = \Delta H - T_m \Delta S. \quad (8)$$

On comparing the activation energy of the main (259°C for CDS free donor and at 305°C for CDS-PA complex) stage of decomposition for the two compounds, the order of the activation energy values is CDS-PA > CDS. This difference may be due to the reactivity, thermal stability of the complex and the new electronic configuration of the PA acceptor attached to CDS. These results agree well with those of the TG analysis detailed above. The  $\Delta S$  values of the main stage for both compounds were found to be negative, indicating that the activated complex is more ordered than the reactants.

**Photostability studies.** Under UV irradiation, it's clear that CDS-PA charge-transfer complex has green fluorescence rather than free CDS ligand itself, supposing that picric acid as acceptor enhances the fluorescence properties of CDS. It is well known that all organic fluorescent compounds undergo bleaching after prolonged exposure to sunlight. A great many fluorescent compounds deteriorate within hours or days in bright sunlight and that, on the other hand, solar collectors are expected to have a lifetime of between 10 and 20 years. The photochemical degradation of CDS and CDS-PA complex doped in PMMA occurs only in the presence of suitable optical radiation (Xenon arc lamp), which produces large local increases in temperature and thermal destruction of the

dye molecules. The CDS and CDS-PA complex doped in PMMA were exposed indoors to UV-Vis radiation and the changes in the absorption spectra achieved at different times during irradiation period are shown in Fig. 8. After complexation the CDS-PA complex demonstrates enhanced photostability. The increasing in photostability is referring to strong chelation between CDS and PA acceptor. The rate constant of photo-degradation of compounds was estimated according to the Eq. (9) [51, 52]:

$$k = \frac{2.303}{t} \log \frac{A_0}{A}, \quad (9)$$

where  $A_0$  and  $A$  are the absorptions before and after irradiation for time ( $t$ ). The  $k$  value and half life times are listed in Table 4. It is clear from the degradation data that the complexation affects the photostability of CDS.

## REFERENCES

1. American Public Health Association, *Standard Methods for the Examination of Water and Wastewater*, 19th ed, Washington, D.C, 1995, p. 3.
2. Lange, B., *Photoelements and Their Applications*, Reinhold Publishing Co. Inc., New York, 1938.
3. Heinisch, G. and Kopelent-Frank, H., in *Progress in Medicinal Chemistry*, Ellis, G.P. and West, G.B., Eds., 1990, vol. 27, p. 141.
4. Heinisch, G. and Kopelent-Frank, H., *Progress in Medicinal Chemistry*, Ellis, G.P. and West, G.B., Eds., 1990, vol. 27, pp. 1–49.



5. Litvinov, V.P. and Dyachenko, V.D., *Russ. Chem. Rev.*, 1997, vol. 66, p. 923.
6. Atanassov, P.K., Linden, A., and Heimgartner, H., *Heterocycles*, 2003, vol. 61, p. 569.
7. Burling, F.T. and Goldstein, B.M., *J. Am. Chem. Soc.*, 1992, vol. 114, p. 2313.
8. Burger, K., Gold, M., Neuhauser, H., Rudolph, M., and Hoess, E., *Synthesis*, 1992, p. 1145.
9. Piatek, M. and Zeslowska, E., *Phosphorus, Sulfur, Silicon Relat. Elem.*, 1996, vol. 117, p. 55.
10. Gasparian, A.V., Yao, Y.J., Liu, J., Yemelyanov, A.Y., Lyakh, L.A., Slaga, J.T., and Budunova, I.V., *Mol. Cancer Ther.*, 2002, vol. 1, p. 1079.
11. Fleming, J., Ghose, A., and Harrison, P.R., *Nutr. Cancer*, 2001, vol. 40, p. 42.
12. Ghose, A., Fleming, J., El-Bayoumy, K., and Harrison, P.R., *Cancer Res.*, 2001, vol. 61, p. 7479.
13. Wu, W., Murakami, K., Koketsu, M., Yamada, Y., and Saiki, I., *Anticancer Res.*, 1999, vol. 19, p. 5375.
14. Hu, C., Zhang, P., Li, H., Ji, Z., and Liu, B., *Huaxue Tongbao*, 2002, vol. 65, p. 162.
15. Koketsu, M., Tanaka, K., Takenaka, Y., Kwong, C.D., and Ishihara, H., *Eur. J. Pharm. Sci.*, 2002, vol. 15, p. 307.
16. Wirth, T., *Tetrahedron*, 1999, vol. 55, p. 1; Petragnani, N., Stefani, H.A., and Valduga, C.J., *Tetrahedron*, 2001, vol. 57, p. 1411.
17. Ishihara, H., Koketsu, M., Fukuta, Y., and Nada, F., *J. Am. Chem. Soc.*, 2001, vol. 123, p. 8408.
18. Koketsu, M., Yang, H.O., Kim, Y.M., Shihashi, M.I., and Shihara, H.I., *Org. Lett.*, 2001, vol. 3, p. 1705.
19. Koketsu, M. and Ishihara, H., *Curr. Org. Chem.*, 2003, vol. 7, p. 175.
20. Hamed, M.M.A., Abdel-Hamid, M.I., and Mahmoud, M.R., *Monatsh. Chem.*, 1998, vol. 129, p. 121.
21. Dozal, A., Keyzer, H., Kim, H.K., and Way, W.W., *Int. J. Antimicrob. Agent*, 2000, vol. 14, p. 261.
22. Mulliken, R.S., *J. Am. Chem. Soc.*, 1950, vol. 72, p. 600.
23. Mulliken, R.S., *J. Am. Chem. Soc.*, 1952, vol. 74, p. 811.
24. Kosower, E.M., *Prog. Phys. Org. Chem.*, 1965, vol. 3, p. 81.
25. Fla, F.P., Palou, J., Valero, R., Hall, C.D., and Speers, P., *JCS Perkin Trans.*, 1991, vol. 2, p. 1925.
26. Roy, T., Dutta, K., Nayek, M.K., Mukherjee, A.K., Banerjee, M., and Seal, B.K., *JCS Perkin Trans.*, 2000, vol. 2, p. 531.
27. Ranby, B. and Rabek, J., *Photodegradation, Photo-oxidation and Photostabilization of Polymers*, London: Wiley, 1975.
28. Crawford, J.C., *Prog Polym Sci.*, 1999, vol. 24, no. 1, p. 7.
29. Abdel-Hafez, Sh.H., *Eur. J. Med. Chem.*, 2008, vol. 43, p. 1971.
30. Refat, M.S., Saad, H.A., and Adam, A.A., *J. Mol. Str.*, 2011, vol. 995, nos. 1–3, p. 116.
31. Skoog, D.A., *Principle of Instrumental Analysis*, 3rd ed., New York: Saunders College Publishing, 1985, ch. 7.
32. Abu-Eittah, R. and Al-Sugeir, F., *Can. J. Chem.*, 1976, vol. 54, p. 3705.
33. Tsubomura, H. and Lang, R.P., *J. Am. Chem. Soc.*, 1964, vol. 86, p. 3930.
34. Kiefer, W. and Bernstein, H.J., *Chem. Phys. Lett.*, 1972, vol. 16, p. 5.
35. Andrews, L., Prochaska, E.S., and Loewenschuss, A., *Inorg. Chem.*, 1980, vol. 19, p. 463.
36. Kaya, K., Mikami, N., Udagawa, Y., and Ito, M., *Chem. Phys. Lett.*, 1972, vol. 16, p. 151.
37. Rathone, R., Lindeman, S.V., and Kochi, J.K., *J. Am. Chem. Soc.*, 1997, vol. 119, p. 9393.
38. Briegleb, G., *Z. Angew. Chem.*, 1964, vol. 76, p. 326.
39. Aloisi, G. and Pignataro, S., *J. Chem. Soc. Faraday Trans.*, 1972, vol. 69, p. 534.
40. Briegleb, G. and Czekalla, J., *Z. Physikchem.*, 1960, vol. 24, p. 237.
41. Martin, A.N., Swarbrick, J., and Cammarata, A., *Physical Pharmacy*, 3 ed., Philadelphia, PA: Lee and Febiger, 1969, p. 344.
42. Witkop, B. and Patrick, J.B., *J. Am. Chem. Soc.*, 1951, vol. 73, p. 713, 1558.
43. Socrates, G., *Infrared Characteristic Group Frequencies*, 1 ed., New York: John Wiley, 1980.
44. Nakanishi, K. and Solomon, P.H., *Infrared Absorption Spectroscopy*, 2 ed., USA, Holden-Day, 1977.
45. Nakamoto, K., *Infrared and Raman Spectra of Inorganic and Coordination Compounds, Part A: Theory and Applications in Inorganic Chemistry*, 6 ed., New York: John Wiley, 2009.
46. Juchnovski, I.N. and Binev, A.G., *J. Organomet. Chem.*, 1975, vol. 99, p. 1.
47. Jensen, K.A., Dahl, B.M., Nielsen, P.H., and Borch, G., *Acta Chem. Scand.*, 1971, vol. 25, p. 2039.
48. Kinugasa, T. and Nakajima, R., *Nippon Kagaku Zasshi*, 1961, vol. 82, p. 1473.
49. Coats, A.W. and Redfern, J.P., *Nature*, 1964, vol. 201, p. 68.
50. Horowitz, H.H. and Metzger, G., *Anal. Chem.*, 1963, vol. 35, p. 1464.
51. Grabchev, I. and Bojinov, V., *Polym. Degrad. Stab.*, 2000, vol. 70, p. 147.
52. Grabchev, I. and Bojinov, V., *Polym. Degrad. Stab.*, 2001, vol. 74, p. 543.